

Accepted Manuscript

Novel π -conjugated molecules based on diimidazopyridine: Significantly improved the photophysical, thermal and electrochemical properties bearing different aryl substituents

Xin Huang, Jinchang Tian, Feng Xu, Xiaochong Liu, Yuqin Li, Yanyan Guo, Wenyi Chu, Zhizhong Sun

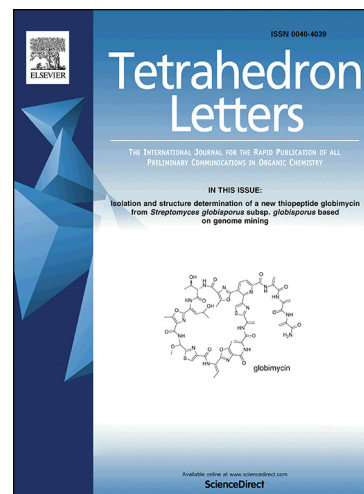
PII: S0040-4039(18)30027-3
DOI: <https://doi.org/10.1016/j.tetlet.2018.01.015>
Reference: TETL 49602

To appear in: *Tetrahedron Letters*

Received Date: 17 November 2017
Revised Date: 25 December 2017
Accepted Date: 5 January 2018

Please cite this article as: Huang, X., Tian, J., Xu, F., Liu, X., Li, Y., Guo, Y., Chu, W., Sun, Z., Novel π -conjugated molecules based on diimidazopyridine: Significantly improved the photophysical, thermal and electrochemical properties bearing different aryl substituents, *Tetrahedron Letters* (2018), doi: <https://doi.org/10.1016/j.tetlet.2018.01.015>

This is a PDF file of an unedited manuscript that has been accepted for publication. As a service to our customers we are providing this early version of the manuscript. The manuscript will undergo copyediting, typesetting, and review of the resulting proof before it is published in its final form. Please note that during the production process errors may be discovered which could affect the content, and all legal disclaimers that apply to the journal pertain.





ELSEVIER

Contents lists available at ScienceDirect

Tetrahedron Letters

journal homepage: www.elsevier.com



Novel π -conjugated molecules based on diimidazolepyridine: Significantly improved the photophysical, thermal and electrochemical properties bearing different aryl substituents

Xin Huang^{a,b}, Jinchang Tian^{a,b}, Feng Xu^{a,b}, Xiaochong Liu^{a,b}, Yuqin Li^{a,b}, Yanyan Guo^{a,b}, Wenyi Chu^{a,b,*}, Zhizhong Sun^{a,b,*}

^a School of Chemistry and Materials Science, Heilongjiang University, Harbin 150080, P. R. China

^b Key Laboratory of Chemical Engineering Process & Technology for High-efficiency Conversion, College of Heilongjiang Province, Harbin 150080, P. R. China

ARTICLE INFO

Article history:

Received

Received in revised form

Accepted

Available online

Keywords:

Diimidazolepyridine derivatives

Suzuki coupling reaction

Cyclization reaction

Blue light emission

ABSTRACT

A series of π -conjugated molecules based on diimidazolepyridine derivatives were designed, synthesized by Suzuki coupling reaction and cyclization reaction and characterized. Diimidazolepyridine motif as the main structure could improve the thermal stability and optical property of the materials. All of the target compounds exhibited good thermal stabilities with T_d values in the range of 416–490 °C. These compounds showed steady blue light emissions in the range of 424–478 nm and high quantum yields (0.33–0.69) in solution. Especially, compound **4f** achieved appropriate energy gap ($E_g=2.69\text{eV}$) and high fluorescence quantum yields ($\Phi_f=0.69$) because of introducing electron-donating group, such energy gap was helpful to electronic transfer and transport. The materials have great potential for good electronic-transmission materials in OLEDs.

1. Introduction

Organic light-emitting diodes (OLEDs) have gained considerable attention owing to their potential applications in solid-state lightings, flexible panel and full-color displays [1–4]. The OLEDs based on small molecules exhibited a lot of advantages as low-energy consumption[5], compatibility with flexible substrates [6], high color rendering index, high contrast and wide viewing angles. Therefore, numerous building blocks such as: biphenyl [7,8], carbazole [9,10], triphenylamine [11–13], anthracene [14,15], and fluorine [16–18] are usually introduced to the structures of OLED blue lighting materials. Most of them possessed non-planar molecular structures that made them difficult to aggregation in the solid state due to dipole-dipole interaction or intermolecular π - π stacking. Thence, they are not conducive to efficient charge injection and transmission in OLED devices. And it is still a great significance to seek excellent performance blue-light emitting materials not only in basic theory but also in applications of device.

Recently, fluorescent materials containing imidazole ring have attracted more attention [19–22]. Because the imidazole derivatives are non-centrosymmetric structures and their conjugated systems can tolerate strong electron-withdrawing/donating groups, imidazole derivatives become potentially useful in electrical and optical materials with high oxidation and reduction potential, chemical stability and thermal decomposition temperature. H. Huang [23] demonstrated the realization of excellent OLEDs based on a high-performance, stable and readily processable electron-transporting phenanthro[9,10-d]imidazole compounds. However, the intrinsic

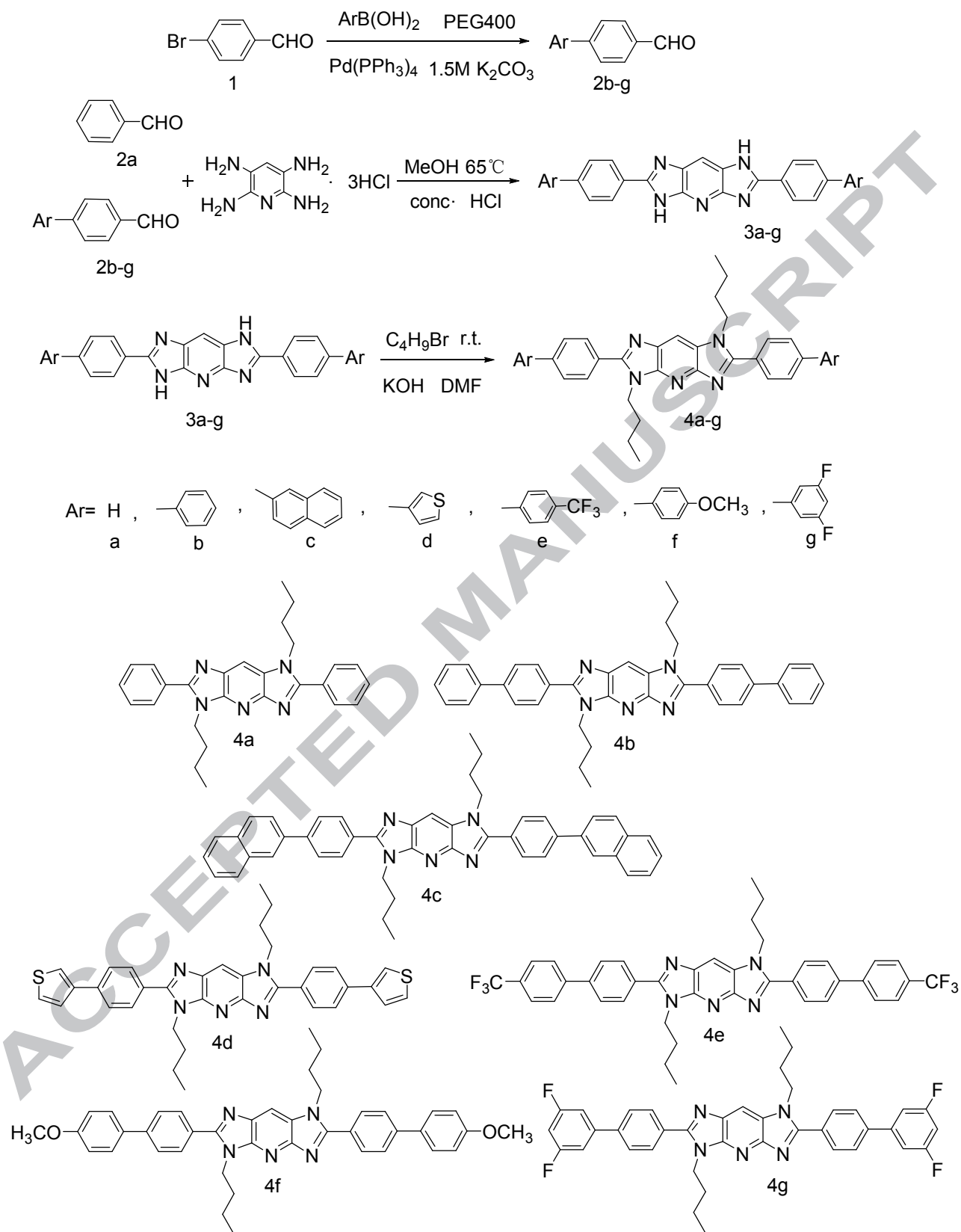
wide energy gaps ($\geq 3\text{ eV}$) of these materials resulted in higher charge-injection barriers and inferior electrical properties [24,25]. As an improvement, R. Zhong [26,27] introduced a pyridine group into the imidazole host structure, which not only improved the thermal stability of the compound but also enhanced the electron-transport properties. Therefore, the compounds containing imidazole and pyridine rings can improve the photoelectric properties and have good application prospects.

In this work, a series of novel diimidazolepyridine were initially designed and synthesized. Wherein, diimidazolepyridine as a condensed unit of diimidazole and pyridine was used as the core backbone, and then different aryl-substitutes were introduced to improve their photoelectric properties. Similarly, two butyl groups were introduced to the N-1/5 positions of the imidazole to increase solubility and released intramolecular π - π stacking. Their structures were characterized by ^1H NMR, ^{13}C NMR and mass spectrometry. Their properties were studied which included thermal analysis, UV absorption spectra, fluorescence emission spectra and the electron-transport ability of the materials in experiment and theory calculation.

[a] School of Chemistry and Materials Science, Heilongjiang University,
Harbin 150080, P. R. China
E-mail: wenyichu@hlju.edu.cn

[b] Key Laboratory of Chemical Engineering Process & Technology for High-efficiency Conversion,
College of Heilongjiang Province, Harbin 150080, P. R. China

* Corresponding author. Tel.: +86-451-86609135; fax: +86-451-86609135; e-mail: wenyichu@hlju.edu.cn



Scheme 1. The synthetic routes of compounds 4a-g

2. Experimental Section

2.1 Materials and Measurements

All starting materials were purchased from TCI; the reagents were obtained from J&K Chemical Company and used without further purification. Synthetic process of materials was monitored by thin layer chromatography (TLC), and the materials were purified by column chromatography carried out on silica gel (200 ~ 300 mesh). ^1H NMR and ^{13}C NMR spectra were recorded on a Bruker DRX 400 MHz and 100 MHz spectrometer in CDCl_3 or DMSO. Chemical shifts were reported in ppm with tetramethylsilane (TMS) as internal standard, and coupling constants (J) were reported in Hertz (Hz). High resolution mass spectra were recorded on Agilent 1100 (VL) mass spectrometer.

Thermogravimetric (TGA) measurements were performed on Shimadzu DTG-60 A thermal analyzers at a heating rate of $10^\circ\text{C}/\text{min}$ under nitrogen atmosphere. UV-visible spectra and photo-luminescence (PL) spectra were measured by Shimadzu UV-2501PC UV-visible spectrophotometer and Shimadzu RF-5301PC fluorescence spectrophotometer, respectively. Cyclic voltammetric (CV) measurements were carried out on the Chi 1200A system in a conventional three-electrode cell with a glass carbon working electrode, a platinum-wire counter electrode and a Ag/AgCl reference electrode referenced in anhydrous dichloromethane solution of $\text{C}_{16}\text{H}_{36}\text{ClNO}_4$ (0.10 M) at a sweeping rate of $100\text{ mV}/\text{s}$ at room temperature. Density functional theory (DFT) calculations were applied to characterize the frontier molecular orbital energy levels of the compounds at the B3LYP/6-31G(d) level by using the Gaussian 03 program. Melting points were measured on a digital melting point apparatus without correction. Infrared spectroscopy (IR) was measured by SP-100 Fourier transform infrared spectroscopy.

2.2 Synthesis of materials

Main synthetic routes of diimidazolepyridine derivatives were shown in **Scheme 1**. To begin our study, 4-bromobenzaldehyde was selected as the starting material. The 4-arylbenzaldehydes (**2b-2g**) were obtained by Suzuki coupling reaction. Intermediates (**3a-3g**) were synthesized by refluxing cyclization of compounds **2a-2g** with 2, 3, 5, 6-tetraaminopyridine trihydrochloride under acidic condition in methanol solution. Finally, the target products (**4a-4g**) were obtained by alkylation reaction with 1-bromobutane under basic condition.

3. Results and Discussion

3.1. Theoretical calculations

For better understanding the structure-property relationship of the diimidazolepyridine derivatives, the molecular configuration and the frontier molecular orbital energy levels were determined using DFT at the B3LYP/6-31G(d) level in the Gaussian 03 software. The results of HOMO and LUMO distribution of these seven compounds were shown in **Fig.1**. Their computed frontier orbital energies were shown in **Table 1**.

As shown in the **Fig.1**, the optimized structures of these derivatives revealed that the diimidazolepyridine derivatives had axial aryl substituents. Such structural features could influence the electrochemical and physicochemical properties. The HOMO and LUMO of the compounds were all populated on the central diimidazolepyridine. But it was found that the LUMO levels were also located over the conjugate parts and electron withdrawing groups. The HOMO levels were also located over the electron-donating group. Obviously, by changing the substituents, a large difference of electronic density was found.

In addition, it could be clearly observed molecular orbital energy level changed by introducing different substituents. Compared with the compound **4a**, introduction of benzene, naphthalene and thiophene groups to the para-position of phenyl (**4b**, **4c** and **4d**) could effectively extend the conjugate chain. It could increase HOMO level and decrease LUMO level. The $\pi-\pi^*$ transition energy would reduce and cause the band bathochromic shift in the absorption and emission spectrum [28]. Simultaneously, introducing strong electronegative groups into the compounds could reduce the HOMO and LUMO levels of the compounds, but the effect of LUMO was more obvious, thus a red-shift of the absorption band was caused [29]. In contrast, the introduction of electron-donating group into the compounds could significantly elevate the HOMO and alter the LUMO moderately. There was considerable electronic coupling between the electron-donating group and the diimidazolepyridine core, thus decreasing the HOMO-LUMO energy gaps and causing red-shift of **4f**. [30] The HOMO-LUMO energy gaps of these compounds were ranged from 2.89 to 3.23 eV. The wide energy gap of **4f** was higher than **4e** and **4g**, and this could be explained that the strong electron-donating substituents reduced the oxidation resistance of the molecule. So combining with the electron acceptor core and electron donor substituent ($-\text{OCH}_3$) could allow the electronic directional movement and be helpful to electronic transfer and transport. [31]

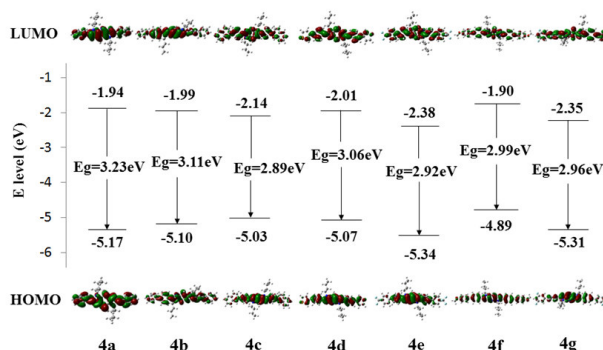


Fig.1. Spatial distributions of frontier orbitals of the target compounds at the B3LYP/6-31G(d) level

3.2 Thermal analysis

The thermal stabilities of the target compounds were determined by thermogravimetric analysis (TGA) in N_2 atmosphere and data were shown in **Fig. 2** and **Table 1**. Decomposition temperatures (T_d , corresponding to 5% weight loss) were measured to be 416, 443, 490, 458, 463, 484 and 467°C for **4a-g**, respectively. The thermodynamic data demonstrated that the T_d values of **4b-g** were higher than **4a**, it was mainly related to the introduction of different aryl substituents. The T_d value of compound **4c** was higher than **4b** and **4d**. Thence, the T_d values increased with the increase of their rigid structure and conjugation degree [32]. In addition, compared with **4b**, the T_d values of **4e**, **4g** and **4f** were increased by 20, 24 and 41°C , respectively. The reason is that introducing substituents into the target compounds led to an increase in molecular weights. This would increase the energy required for molecular cleavage to result in an increase of T_d values. Moreover, the melting points (T_m) of these compounds were 181, 229, 261, 252, 244, 236 and 213°C , respectively. The T_m s of **4b-4g** were higher than **4a**, this is due to the introduction of different aryl substituents which made the molecular weight increase, then resulted in an increase in the intramolecular $\pi-\pi$ interactions. Therefore, these compounds showed good thermal stability.

Table 1. E_{ox} , E_g , E_{HOMO} , E_{LUMO} and physical properties of the target compounds

Compound	Band gap ^a	HOMO/LUMO ^a (eV)	E_g^b	E_{ox}^c (V)	E_{HOMO}/E_{LUMO}^d (eV)	T_d^e/T_m^e (°C)	λ_{max}^{Abs} (nm)		λ_{max}^{PL} (nm)		Φ^h
							Solution ^f	Film ^g	Solution ^f	Film ^g	
4a	3.23	-5.27/-2.04	2.90	0.68	-5.48/-2.58	416/181	306,391	269,403	424	528	0.33
4b	3.11	-5.20/-2.09	2.79	0.62	-5.42/-2.63	443/229	271,408	261,410	462	532	0.55
4c	2.89	-5.13/-2.24	2.67	0.57	-5.37/-2.70	490/261	251,412	256,412	469	563	0.56
4d	3.06	-5.17/-2.11	2.72	0.61	-5.41/-2.69	458/252	279,415	279,414	464	567	0.43
4e	2.92	-5.44/-2.52	2.78	0.95	-5.75/-2.97	463/244	274,406	271,408	445	550	0.42
4f	2.99	-4.99/-2.00	2.69	0.46	-5.26/-2.57	484/236	281,417	278,415	478	562	0.69
4g	2.96	-5.41/-2.45	2.77	0.84	-5.64/-2.87	467/213	268,404	274,405	466	531	0.67

[a] DFT/B3LYP calculated values. [b] Optical energy gaps calculated from the edge of the electronic absorption band rate of 100 mV s⁻¹. [c] Oxidation potential in CH₂Cl₂ (10⁻³ M) containing 0.1 M (n-C₄H₉)₄NPF₆ with a scan rate of 100 mV s⁻¹. [d] Measured by Cyclic voltammogram. [e] Obtained from TGA measurements with a heating rate of 10 °C/min under N₂. [f] Measured in a dilute CH₂Cl₂ solution (10⁻³ M). [g] Measured in solid films. [h] Measured in CH₂Cl₂ with quinine sulfate as the standard.

It was obvious that the T_d values of the diimidazolepyridine derivatives were higher than the reported benzimidazole derivatives [33] which synthesized with a single imidazole ring. The π -conjugation and thermal stability were improved owing to the main structure which contained two imidazole groups. So diimidazolepyridine derivatives had great potential to fabricate into devices by vacuum thermal evaporation technology.

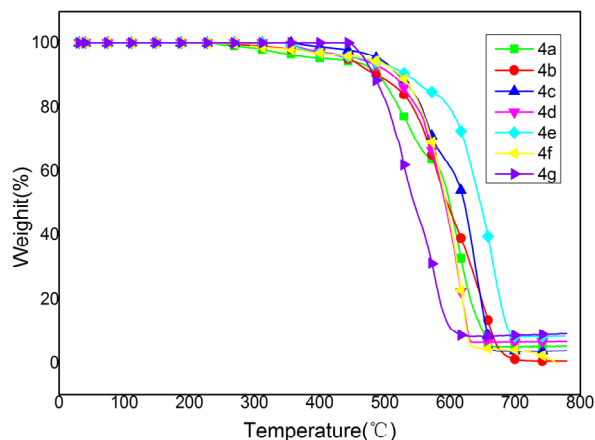


Fig.2. TGA graphs of target compounds recorded at a scanning rate of 10 °C/min.

3.3. Photophysical properties

The UV-visible absorption and photoluminescence (PL) of these compounds in CH₂Cl₂ dilute solution and solid films were shown in **Fig. 3**, and the spectral parameters were summarized in **Table 1**.

As shown in **Fig. 3(a)(c)**, the similar spectral patterns of different derivatives were observed. Due to the similar structure, these compounds exhibited two similar UV absorption bands in solution and solid film at wavelength about 270 and 410 nm, corresponding to $n-\pi^*$ and $\pi-\pi^*$ transitions of diimidazolepyridine and $\pi-\pi^*$ transition of aryl substituents.[34] However, compared with the compound **4b**, there was a slightly blue-shift in the peak maximum of the compounds **4e** and **4g**. According to the Hammett constants, the substituent constants (σ)[35] (**Fig.S29**) are known that the p -CF₃ and m -F groups are

evidently electron-withdrawing substituents ($\sigma=+0.54/+0.34$). The introduction of -CF₃ and -F showed the electron-withdrawing inductive effect, which reduced the electron cloud density of the conjugation system and increased the transition energy of the whole system, then resulted in blue shift. Otherwise, the compound **4f** showed a pronounced bathochromic shift of the $\pi-\pi^*$ band. The p -OMe group is evidently electron-donating substituent ($\sigma=-0.27$). The introduction of -OCH₃ showed the electron-donating conjugated effect, which increased the electron cloud density of the conjugation system and reduced the transition energy of the whole system, then resulted in red shift. Moreover, compared to the **4a**, with increasing the π -conjugation of the compounds **4b-d**, the corresponding $\pi-\pi^*$ electron transition energy level would be decreased and caused the whole absorption spectrum red-shift [36]. The optical band gaps (E_g) of the target compounds, which were calculated from the absorption edges (λ_{on}) of the UV-vis absorption spectra in the dilute CH₂Cl₂ solution with a formula $E_g=1240/\lambda_{on}$. They were 2.90, 2.79, 2.67, 2.72, 2.78, 2.69 and 2.77 eV, respectively[37].

As shown in **Fig. 3(b)**, significant solvatochromic behaviors were observed with remarkable red-shifts (408-428nm) of the maximal absorption band for the compound **4f** from the toluene to methanol. With the increasing of the polarity of the solvent, the polarity of the excited state was greater than that of the ground state, which resulted in a large degree of energy reduction of the excited state. The gap between the ground state and the excited state would be decreased. Then, the transition ability became larger, which was beneficial to the intramolecular charge transfer. [38,39] Meanwhile, these compounds exhibited good solubility in different solvents.

As shown in **Fig. 3(d)**, the photoluminescence (PL) spectra of all the synthesized materials were highly emissive in CH₂Cl₂ solution with emission maxima focusing on the blue light region of 424-478 nm. The PL maxima of the compounds **4b-d** were red-shifted by 38-45 nm relative to that of the compound **4a** because of extending the conjugation length. [40] Compared with the electron-withdrawing derivatives (-CF₃ and -F), the electron-donating derivative (-OCH₃) occurred red-shift obviously due to the increase in the degree of intramolecular charge transfer. As shown in **Fig. 3(e)**, by comparison with the emission spectra in the dilute solution, the solid-state emissions were red-shifted in the range of 65-105nm. The reason is that intermolecular $\pi-\pi$

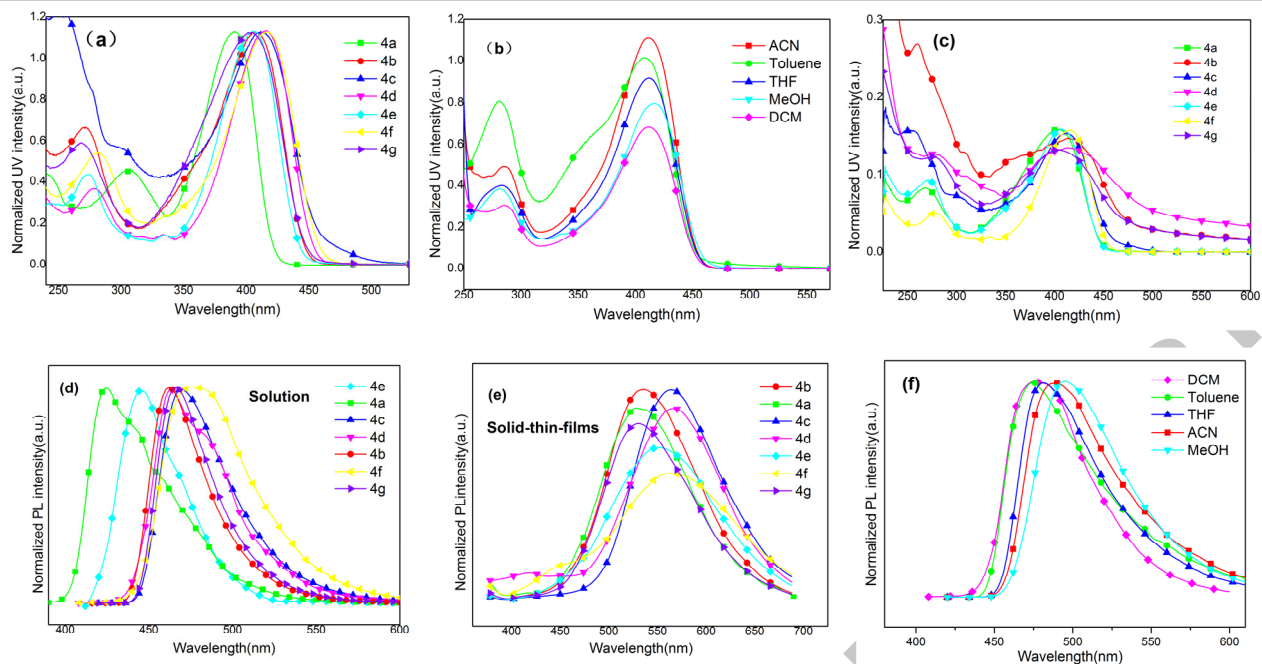


Fig.3. (a) UV-vis absorption in CH_2Cl_2 solution (10^{-5} M) of diimidazolepyridine derivatives. (b) UV-vis absorption in different solution of **4f**. (c) UV-vis absorption in solid films. (d) PL spectra in CH_2Cl_2 solution (10^{-5} M). (e) PL spectra in solid films. (f) PL spectra in different solution of **4f**.

stacking increased intermolecular forces, reduced twist, enhanced the coplanarity and the conjugation degree. [41] Simultaneously, these diimidazolepyridine derivatives presented the intermolecular interactions, originating due to the specific molecular packing of the planar molecular configuration and making them easy to aggregate in the solid state. [42] As shown in **Fig. 3(f)**, significant solvatochromism behaviors were also observed with remarkable red-shifts (474-495nm) of the PL spectra for the compound **4f** from the toluene to methanol. This indicates the occurrence of charge transfer upon photoexcitation.

Contrast to the reported 6,10-dihydrofluoreno[2,3-d:6,7-d']diimidazole derivatives[43], the PL spectra of diimidazolepyridine derivatives in solution and in the solid state occurred red-shift. This indicated the fusion of electron acceptor pyridine with high electron affinity made the intramolecular charge-transfer greatly enhanced. [44] The emission images of the materials in CH_2Cl_2 under irradiation at 365 nm under room temperature were shown in **Fig. 4**. All compounds exhibited blue light emission stably. Therefore, these compounds had the potential to be used as fluorescent materials.



Fig.4. The emission images at 365 nm UV illuminations.

In order to further understand the emission property of these diimidazolepyridine derivatives, fluorescence quantum yields (FQY) of all of the blue materials were evaluated using quinine sulfate in 0.01 M H_2SO_4 solution ($\Phi_f=0.55$) as the calibration

standard [45], and the results were summarized in **Table 1**. The experimental results indicated these compounds exhibited relatively high FQY in dilute CH_2Cl_2 solution. The FQYs of them were 0.33, 0.55, 0.56, 0.43, 0.42, 0.69 and 0.67, respectively. The results also indicated that the fluorinated compound and electron-donating substituted compound in periphery exhibited the high FQY since the twisted and rigid configuration could reduce the nonradiative decay. [46]

3.4. Electrochemical properties

To further evaluate the feasibility of the new materials in the field of optoelectronic applications, the electrochemical behaviours of the compounds **4a-g** were explored by cyclic voltammetry (**Fig.5**) and the data were listed in **Table 1**. As shown in **Fig.5**, these seven materials revealed seven irreversible anode peaks of the initial oxidation characteristic and seven irreversible cathodic peaks of the initial reduction feature. The onset oxidation peaks (E_{ox}) for the compounds **4a-g** were from 0.46 to 0.95 V (versus the ferrocenium/ferrocene redox couple). Using Ag/AgCl as the reference electrode the HOMO levels were calculated according to the following formula ($E_{HOMO} = -(E_{ox} + 4.8)$ eV). The HOMOs were in the range of -5.26 to -5.75 eV, while the LUMOs were in the range of -2.57 to -2.97 eV by the formula ($E_{LUMO} = -(E_{HOMO} + E_g)$)[47]. This trend was in good consistent with the calculated values (the HOMOs were in the range of -4.99 to -5.44 eV and the LUMOs were in the range of -2.00 to -2.52 eV). The results showed that the similar voltammograms were obtained for all target compounds.

Compared to the only phenyl-substituted compounds **4a**, it could be rationalized that the increasing conjugation might reduce the oxidation potentials of the molecule and made the LUMO energy level decrease by 0.05, 0.12 and 0.11 eV (**4b-d**), respectively. Lower LUMO levels reduced the energy barriers between electron-transport and emitting layers and would facilitate electron-injection into the emission layers. [48] In addition, the introduction of electron-donating groups in the compound **4f** made the HOMO/LUMO energy levels increase by

0.22/0.01 eV. And it showed the HOMO/LUMO energy levels of **4f** were higher than that of **4a**. The results were consistent with the DFT calculation. And the introduction of electron-withdrawing groups at the para-position of the aryl rings (**4e**, **4g**) could decrease the HOMO/LUMO energy levels by 0.27/0.39 and 0.16/0.29 eV, respectively.

Specifically, thermodynamic stability requires that the electrode electrochemical potentials μ_A and μ_C (anode and cathode electrochemical potentials μ_A and μ_C (vs E_{ox} and E_{red})) are locating in the window of the electrolyte ($\mu_A - \mu_C \leq E_g$). The reduction potentials (E_{red}) for the compounds **4a-g** from CV curves were -1.89, -2.03, -1.85, -1.76, -1.68, -1.97 and -1.63 eV, respectively. Taking the compound **4f** as an example: $\mu_A - \mu_C = 0.46 - (-1.97) = 2.43 \leq E_g$ (2.69). Therefore, an anode and a cathode with their μ_A and μ_C values well-matched to the window of the electrolyte (E_g) could demonstrate these compounds good thermodynamic stability. [49]

It was found that all compounds had lower LUMO levels than the widely used electron-transport material 8-hydroxyquinoline aluminum (Alq_3 , -1.86 eV), indicating that they have higher electron affinity than Alq_3 . Therefore, these compounds can be used as the OLEDs due to their good electron-transport properties. [50]

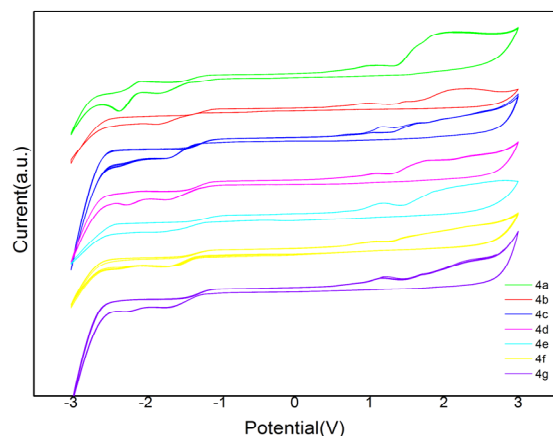


Fig.5. The CV curves of compounds **4a-g** in the solution of CH_2Cl_2

4. Conclusions

Seven kinds of diimidazolepyridine derivatives with donor-acceptor-donor systems were designed and synthesized. Their structures were confirmed by 1H NMR, ^{13}C NMR, HRMS, UV and IR. Their thermal, optical and electrochemical properties were investigated, and the results indicated that the photoelectric characteristics of the target compounds showed dependence on their molecular structure. For diimidazolepyridine motif as the main structure, the introduction of biimidazole could improve the thermal stability of the materials, resulting in T_d values exceeding 416 °C, or even up to 490 °C (**4c**). Moreover, the fusion of electron acceptor pyridine unit enhanced the intramolecular charge-transfer and enabled the emission wavelength in the range of 424–478nm. The introduction of the dibutyl chain also enhanced the solubility of the compounds. Furthermore, introducing electron-donating group (**4f**) improved the electron transport properties of the electron-acceptor core and achieved appropriate energy gap ($E_g=2.69$ eV) and high fluorescence quantum yields ($\Phi_f=0.69$). Therefore, these compounds have great potential for electron-transporting materials in OLEDs.

Further research about these new compounds used as blue light-emitting materials is presently under studied in our laboratory.

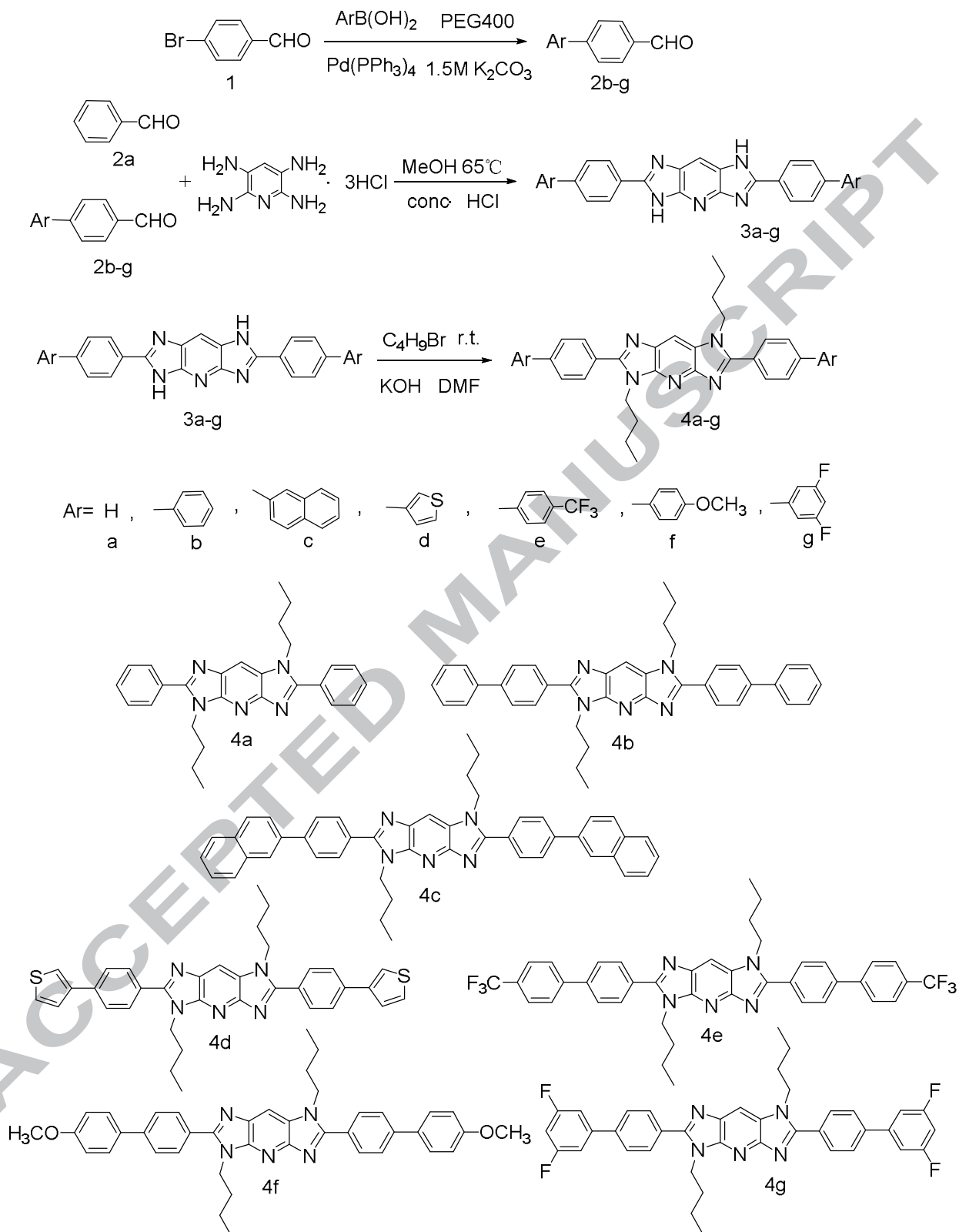
Acknowledgments

We are grateful for financial support from the Research Project of the Natural Science Foundation of Heilongjiang Province of China (No. B201207 and No. B201208).

References

- [1] Shih PI, Chuang CY, Chien CH, et al. *Adv Funct Mater.* 2007; 17: 3141-3146.
- [2] Yang X, Zheng S, Bottger R, et al. *J Phys Chem C.* 2011; 115: 14347-14352.
- [3] Chen YH, Chou HH, Su TH, et al. *Chem Commun.* 2011; 47: 8865-8867.
- [4] Hu JY, Pu YJ, Yamashita Y, et al. *J Mater Chem C.* 2013; 1: 3871-3878.
- [5] Liu J. *Spectrochim Acta A.* 2015; 149: 48-53.
- [6] Tavgeniene D, Krucaite G, Baranauskite U, et al. *Dyes Pigm.* 2017; 137: 615-621.
- [7] Gao W, Wang S, Xiao Y, et al. *Dyes Pigm.* 2013; 97: 92-99.
- [8] Wu Q, Lavigne JA, Tao Y, et al. *Chem Mater.* 2001; 13: 71-77.
- [9] Morin JF, Drolet N, Tao Y, et al. *Chem Mater.* 2004; 16: 4619-4626.
- [10] Gao W, Wang S, Xiao Y, et al. *Spectrochim Acta A.* 2012; 98: 215-221.
- [11] Li Z, Wu Z, Fu W, et al. *J Phys Chem C.* 2012; 116: 20504-20512.
- [12] Sek D, Iwan A, Jarzabek B, et al. *Macromolecules.* 2008; 41: 6653-6663.
- [13] Fan C, Wang X, Luo J. *Opt Mater.* 2017; 64: 489-495. *Dyes Pigm.* 2015; 122: 264-271.
- [14] Song Y, Lee SB, Lee SJ, et al. *Thin Solid Films.* 2015; 577: 42-48.
- [15] Giménez R, Piñol M, Serrano JL. *Chem Mater.* 2004; 16: 1377-1383.
- [16] Jiang Z, Liu Z, Yang C, et al. *Adv Funct Mater.* 2009; 19: 3987-3995.
- [17] Wan W, Du H, Wang J, et al. *Dyes Pigm.* 2013; 96: 642-652.
- [18] Lee HW, Kim HJ, Kim YS, et al. *Displays.* 2015; 39: 1-5.
- [19] Shan T, Liu Y, Tang X, et al. *ACS Appl Mater Inter.* 2016; 8: 28771-28779.
- [20] Irfan M, Ahmad I, Samra SA, et al. *Mater Lett.* 2015; 161: 37-40.
- [21] Dinçalp H, Saltan GM, Aykut D, et al. *Spectrochim Acta A.* 2015; 149: 157-165.
- [22] Subeesh MS, Shanmugasundaram K, Sunesh CD, et al. *J Phys Chem C.* 2016; 120: 12207-12217.
- [23] Huang H, Wang Y, Zhuang S, et al. *J Phys Chem C.* 2012; 116: 19458-19466.
- [24] Chen WC, Yuan Y, Wu GF, et al. *Org Electron.* 2015; 17: 159-166.

- [25] Xu X, Ye S, He B, et al. *Dyes Pigm.* 2014; 101: 136-141.
- [26] Zhong R, Xu S, Wang J, et al. *Spectrochim Acta A.* 2016; 161: 27-32
- [27] Cui Y, Yin YM, Cao HT, et al. *Dyes Pigm.* 2015; 119: 62-69.
- [28] Ouyang X, Li XL, Zhang X, et al. *Dyes Pigm.* 2015; 122: 264-271.
- [29] Dong H, Wang C, Hu W. *Chem Commun.* 2010; 46: 5211-5222.
- [30] Hsieh CP, Lu HP, Chiu CL, et al. *J Phys Chem C.* 2010; 20: 1127-1134.
- [31] Yang S, Guan D, Yang M, et al. *Tetrahedron Lett.* 2015; 56: 2223-2227.
- [32] Li TT, Gao YC, Zhou JX, et al. *RSC Adv.* 2015; 5: 84547-84552.
- [33] Ouyang X, Zhang X, Ge Z. *Dyes Pigm.* 2014; 103: 39-49.
- [34] Guo JG, Cui YM, Lin HX, et al. *J Photoch Photobio A.* 2011; 219: 42-49.
- [35] Hansch C, Leo A, Taft R W. *Chem Rev.* 1991; 91: 165-195.
- [36] Tian J, Yang M, Wang L, et al. *Tetrahedron.* 2017; 73: 230-238.
- [37] Liang W, Gao Z, Song W, et al. *Tetrahedron.* 2016; 72: 1505-1510.
- [38] Rusu E, Dorohoi DO, Airinei A. *J Mol Struct.* 2008; 887: 216-219.
- [39] Wang S, Cheng Z, Song X, et al. *ACS Appl Mater Inter.* 2017; 9: 9892-9901.
- [40] Gao Z, Wang Z, Shan T, et al. *Org Electron.* 2014; 15: 2667-2676.
- [41] Subeesh MS, Shanmugasundaram K, Sunesh CD, et al. *J Phys Chem C.* 2015; 119: 23676-23684.
- [42] Kumar S, Singh P, Kumar P, et al. *J Phys Chem C.* 2016; 120: 12723-12733.
- [43] Chen HF, Cui YM, Guo JG, et al. *Dyes Pigm.* 2012; 94: 583-591.
- [44] Su SJ, Sasabe H, Takeda T, et al. *Chem Mater.* 2008; 20: 1691-1693.
- [45] Velapoldi RA, Tønnesen HH. *J Fluoresc.* 2004; 14: 465-472.
- [46] Zhu M, Ye T, Li CG, et al. *J Phys Chem C.* 2011; 115: 17965-17972.
- [47] Bredas JL, Silbey R, Boudreaux DS, et al. *J. Am. Chem. Soc.* 1983; 105: 6555-6559.
- [48] Ikai M, Tokito S, Sakamoto Y, et al. *Appl Phys Lett.* 2001; 79: 156-158.
- [49] Goodenough JB, Kim Y. *Chem Mater.* 2009; 22: 587-603.
- [50] Jeon SO, Yook KS, Lee JY. *Thin Solid Films.* 2010, 519, 890-893.

Scheme1. The synthetic routes of compounds **4a-g**

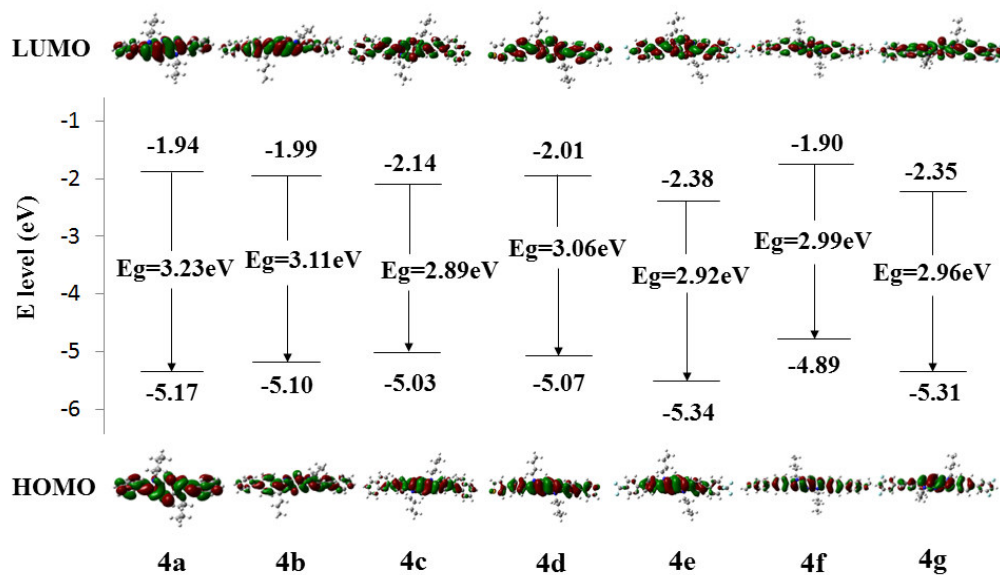


Fig.1. Spatial distributions of frontier orbitals of the target compounds at the B3LYP/6-31G(d) level

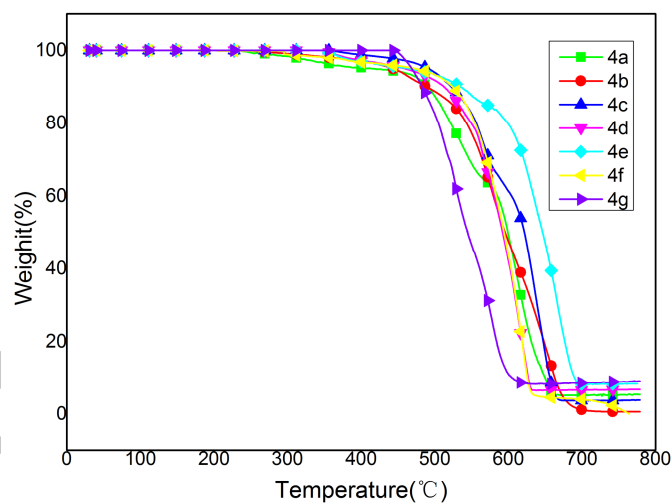
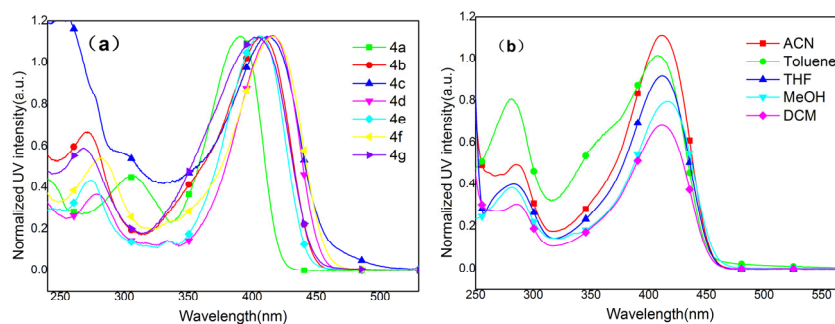


Fig.2. TGA graphs of target compounds recorded at a scanning rate of 10 °C /min.



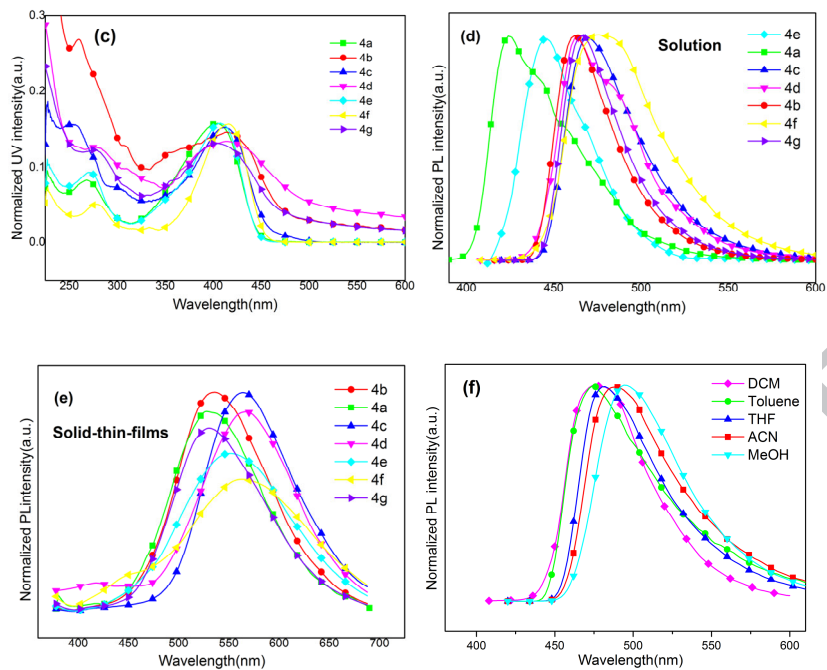


Fig.3. (a) UV-vis absorption in CH₂Cl₂ solution (10^{-5} M) of diimidazolepyridine derivatives. (b) UV-vis absorption in different solution of **4f**. (c) UV-vis absorption in solid films. (d) PL spectra in CH₂Cl₂ solution (10^{-5} M). (e) PL spectra in solid films. (f) PL spectra in different solution of **4f**.



Fig.4. The emission images at 365 nm UV illumination

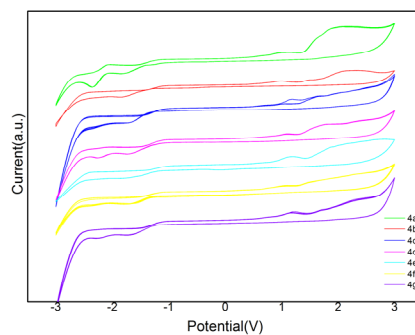
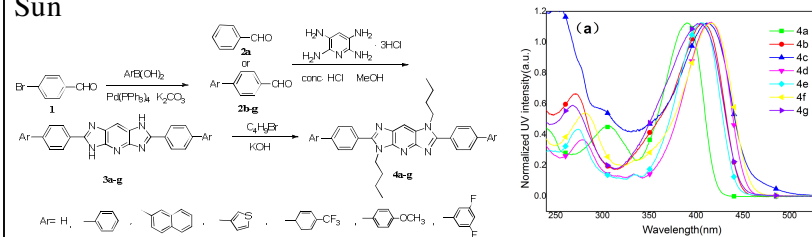


Fig.4. The CV curves of compounds **4a-g** in the solution of CH₂Cl₂.

Graphical Abstract

Novel π -conjugated molecules based on diimidazopyridine: Significantly improved the photophysical, thermal and electrochemical properties bearing different aryl substituents

Xin Huang, Jinchang Tian, Feng Xu, Xiaochong Liu, Yuqin Li, Yanyan Guo, Wenyi Chu^{*}, Zhizhong Sun^{*}



1. Diimidazolepyridine derivatives were designed and successfully synthesized.
2. Diimidazolepyridine motif could improve thermal stability and optical property.
3. Introducing different aryl-substituents to balance charge transfer and prevent to form an "electron trap".
4. These new compounds showed the potential to be used as blue fluorescent materials.

ACCEPTED MANUSCRIPT

Table 1. E_{ox} , E_g , E_{HOMO} , E_{LUMO} and physical properties of the target compounds

Compound	Band gap ^a	HOMO/LUMO ^a (eV)	E_g ^b	E_{ox} ^c (V)	$E_{\text{HOMO}}/E_{\text{LUMO}}^d$ (eV)	T_d^g/T_m^h (°C)	$\lambda_{\text{max}}^{\text{Abs}}$ (nm)		$\lambda_{\text{max}}^{\text{PL}}$ (nm)		Φ_i^h
							Solution ^f	Film ^g	Solution ^f	Film ^g	
4a	3.23	-5.27/-2.04	2.90	0.68	-5.48/-2.58	416/181	306,391	269,403	424	528	0.33
4b	3.11	-5.20/-2.09	2.79	0.62	-5.42/-2.63	443/229	271,408	261,410	462	532	0.55
4c	2.89	-5.13/-2.24	2.67	0.57	-5.37/-2.70	490/261	251,412	256,412	469	563	0.56
4d	3.06	-5.17/-2.11	2.72	0.61	-5.41/-2.69	458/252	279,415	279,414	464	567	0.43
4e	2.92	-5.44/-2.52	2.78	0.95	-5.75/-2.97	463/244	274,406	271,408	445	550	0.42
4f	2.99	-4.99/-2.00	2.69	0.46	-5.26/-2.57	484/236	281,417	278,415	478	562	0.69
4g	2.96	-5.41/-2.45	2.77	0.84	-5.64/-2.87	467/213	268,404	274,405	466	531	0.67

[a] DFT/B3LYP calculated values. [b] Optical energy gaps calculated from the edge of the electronic absorption band rate of 100 mV s⁻¹. [c] Oxidation potential in CH₂Cl₂ (10⁻⁵ M) containing 0.1 M (n-C₄H₉)₄NPF₆ with a scan rate of 100 mV s⁻¹. [d] E_{HOMO} was calculated by $-(E_{\text{ox}} + 4.4)$, and $E_{\text{LUMO}} = -(E_{\text{HOMO}} + E_g)$ [e] Obtained from TGA measurements with a heating rate of 10 °C/min under N₂. [f] Measured in a dilute CH₂Cl₂ solution (10⁻⁵ M). [g] Measured in solid films. [h] Measured in CH₂Cl₂ with quinine sulfate as the standard.